Chapter 5
Aromatics

P. R. van der Linde and H. A. J. Oonk

Abstract A start is made with the family of the *para*-dihalobenzenes, including the key system *p*-dichlorobenzene + *p*-dibromobenzene. Special attention is given to the melting behaviour of mixed materials prepared by zone levelling. The family of the dihalobenzenes is followed by the group of the 2-*R*-substituted naphthalenes which includes naphthalene itself (R = H), and the substances with R = F, Cl, Br, SH, CH_3, and OH. It appears that the naphthalene group falls apart into two structural subfamilies. Furthermore, evidence is given of an extra attractive effect between substituted methyl and substituted halogen. In addition, a number of stand-alone systems are discussed, on the basis of which afore-mentioned phenomena are further illustrated. One of these systems is *trans*-azobenzene + *trans*-stilbene for which the outcome of lattice energy calculations is also presented.

5.1 Introduction

The chapter starts by treating a family of binary systems whose components belong to a *chemically coherent group* of substances: the family of the *para*-dihalobenzenes, with halo = Cl, Br, I. With the exception of the diiodo compound, the members of the family are monoclinic and have the same space group, which is $P2_1/a$. The five members with the same space group comprise ten binary systems; nine of these systems form, at room temperature, a continuous series of mixed crystals. The thermodynamic mixing properties of the ten binary systems are correlated with the *coefficient of crystalline isomorphism*, ε_m. This coefficient expresses the geometric similarity between the unit cells of the constituting components; its value is given by

$$\varepsilon_m = 1 - \frac{\Delta_m}{\Gamma_m} \tag{5.1}$$

P. R. van der Linde (✉) · H. A. J. Oonk
Universiteit Utrecht, Utrecht, The Netherlands
e-mail: petervdl@mac.com

H. A. J. Oonk
e-mail: h.a.j.oonk@uu.nl

M. À. Cuevas-Diarte and H. A. J. Oonk (eds.), *Molecular Mixed Crystals*,
Physical Chemistry in Action, https://doi.org/10.1007/978-3-030-68727-4_5

in which Γ_m is the common (included) volume and Δ_m the excluded volume when the two unit cells are brought to maximal overlap.[1] Special attention is given to the system *p*-dichlorobenzene + *p*-dibromobenzene, which, through the years, has been a key system for the study of mixed crystals.

Next, the group of the 2-*R*-substituted naphthalenes is considered. The members of the group are naphthalene itself (R = H); the halo-substituted members (R = F, Cl, Br, and including R = SH); 2-methylnaphthalene ($R = CH_3$); and 2-naphthol (R = OH). In this case, there are two *structural subfamilies*, and it means that there is a subtle role of *polymorphism*. In addition, and in contrast to the *para*-dihalobenzenes, a number of the naphthalene systems have components that do not belong to a chemically coherent group; this means that their thermodynamic properties are not determined by geometric similarity (i.e. ε_m) alone. This aspect is elaborated for the combinations of naphthalene with 2-fluoronaphthalene and 2-naphthol and the combinations of 2-methylnaphthalene with the 2-halonaphthalenes.

Apart from the two families of systems, a number of stand-alone systems make their appearance. Some of these systems are just mentioned; some others are treated in some detail. The former include 1,3,5-trichlorobenzene + 1,3,5-tribromobenzene and 1,2,4,5-tetrachlorobenzene + 1,2,4,5-tetrabromobenzene. The latter are *trans*-azobenzene + *trans*-stilbene, thiophene + benzene, and thianaphthene + naphthalene.

Throughout the chapter, emphasis is on phenomenology and experimental methodology. Moreover, for the thermodynamic mixing properties of the mixed crystalline state (superscript sol), the *ABΘ model* (see Chap. 3) is adopted. In this model, the molar *excess Gibbs energy*, as a function of temperature T and composition X, is given by

$$G^{E,\mathrm{sol}}(T, X) = A \cdot X \cdot (1 - X) \cdot \left(1 - \frac{T}{\theta}\right) \cdot [1 + B \cdot (1 - 2 \cdot X)]; \qquad (5.2)$$

in which A, B, and Θ are system-dependent parameters; Θ is the so-called *compensation temperature* (see Chap. 3). The composition variable X stands for the mole fraction of the second component. Invariably the second of the two components is the one with the larger molar volume.

The fact that the model expression for G^E is taken linear in temperature implies that the *excess enthalpy*, H^E, is independent of temperature. Hence, the corresponding expression for H^E, the *heat of mixing*, is

$$H^{E,\mathrm{sol}}(T, X) \Rightarrow H^{E,\mathrm{sol}}(X) = A \cdot X \cdot (1 - X) \cdot [1 + B \cdot (1 - 2 \cdot X)]. \qquad (5.3)$$

Note: as for instance shown by van der Linde [1] and Yamamuro et al. [2], molecular systems that form mixed crystals have virtually ideal liquid mixtures. It means that $H^{E,\mathrm{sol}}$ and $G^{E,\mathrm{sol}}$ virtually are equal to *minus* ΔH^E and *minus* ΔG^E, respectively,

[1] A counterpart of ε_m is ε_k, the coefficient of *molecular homeomorphism*. The definition of ε_k is similar to the above definition of ε_m: 'unit cells' has to be replaced by 'molecules' (see also Chap. 2).

where the operator Δ stands for the difference between liquid and solid:

$$\Delta G^E = G^{E,\text{liq}} - G^{E,\text{sol}} \Rightarrow -G^{E,\text{sol}} \tag{5.4}$$

$$\Delta H^E = H^{E,\text{liq}} - H^{E,\text{sol}} \Rightarrow -H^{E,\text{sol}} \tag{5.5}$$

In the text, the *difference properties* ΔG^E and ΔH^E quite often make their appearance, because, strictly speaking, these are the ones that follow from the experimental information.

5.2 The *para*-Dihalobenzene Family

The five substances *p*-dichlorobenzene (ClCl), *p*-bromochlorobenzene (BrCl), *p*-chloroiodobenzene (ClI), *p*-dibromobenzene (BrBr), and *p*-bromoiodobenzene (BrI) are crystalline at room temperature, all having space group $P2_1/a$, with two molecules per unit cell. With the exception for ClCl, the crystal structure remains the same on heating to the melting point. In discussing the binary phase diagrams, the existence of ClCl's polymorphism is ignored; it is discussed in Sect. 5.3.

The five substances include ten binary systems, and from thermal analytical work, it is known, for a long time, that the substances are miscible in the solid state. In the case of nine systems, miscibility is complete; limited miscibility is shown by ClCl + BrI.

In 1991, Calvet et al. [3] presented a study in which for the ten binary systems the change from solid to liquid was investigated by *differential scanning calorimetry (DSC)* and subsequently subjected to a thermodynamic analysis in terms of *LIQFIT* [4]. LIQFIT allows for the calculation of thermodynamic excess functions on the basis of (experimental) liquidus data. The outcome of the study is summarized in Table 5.1.

At the time of writing the 1991 paper, there was some confusion about the nature of the solid state, evoked by X-ray observations that could be taken as evidence of a demixing phenomenon; see e.g. Haget et al. [5]. In Table 5.1, the systems that were suspected of demixing have numbers marked with an asterisk. Today, it is known that the X-ray observations are in conflict with the state of true equilibrium, read minimal Gibbs energy. In the case of the system ClCl + BrI, with its eutectic phase diagram, there is a thermodynamically real *miscibility gap* [8].

Notwithstanding the experimental uncertainties in measured enthalpy effects and computed excess Gibbs energies, the information contained in Table 5.1 gives evidence of two important facts.

In the first place, as follows from Fig. 5.1, the equimolar excess Gibbs energy effect of the mixed crystalline state (from the available data calculated for $T = 333$ K) is proportional to the equimolar excess enthalpy effect. This observation is evidence of the fact that the systems correspond to a *class of similar systems* in terms

Table 5.1 Results of a thermodynamic analysis of ten binary *para*-dihalobenzene systems: equimolar excess enthalpy differences (ΔH^E) and excess Gibbs energy differences (ΔG^E) at the mean temperature of the solid-liquid region (T_{mean}) [3], along with the geometric mismatch between the components in terms of the coefficient of crystalline isomorphism ε_{m} [6] and the type of phase diagram.

System	Number	$(1-\varepsilon_{\text{m}})$	Type	T_{mean} (K)	$-\Delta H^E(X=0.5)$ (J mol^{-1})	$-\Delta G^E(X=0.5)$ (J mol^{-1})
ClCl + BrCl	1	0.033	[0]/[–]	329	220	120
ClCl + BrBr	2*	0.064	[0]/[–]	338	1090	360
ClCl + ClI	3	0.121	[–]	312	2230	720
ClCl + BrI	4	0.143	[e]	312	1990	850
BrCl + BrBr	5	0.029	[0]/[–]	346	130	170
BrCl + ClI	6	0.085	[–]	326	980	330
BrCl + BrI	7*	0.107	[–]	340	1960	540
BrBr + ClI	8*	0.054	[0]	341	760	110
BrBr + BrI	9	0.075	[–]	356	1100	290
ClI + BrI	10*	0.020	[0]	343	520	50

The asterisks in the second column refer to systems that were suspected of showing demixing phenomena.
For types of phase diagram and the symbols used in the fourth column, see Oonk and Calvet [7]. The indication [0]/[–] is for systems that (tend to) have a minimum close to the melting point of the lower melting component. ClCl's polymorphism is ignored.
(adapted from Ref. [3], © 1991, with permission from Elsevier)

of *enthalpy/entropy compensation* (see Chap. 3). The compensation temperature that corresponds to the diagonal in Fig. 5.1 is $\Theta = 500$ K.

The second fact, more obvious than the first, is that the equimolar excess enthalpy effect increases with decreasing geometric similarity (ε_{m}) between the components of the member system; see Fig. 5.2.

5.3 Polymorphism of *p*-Dichlorobenzene

The substance *p*-dichlorobenzene has three solid forms, which are in order of their appearance on the temperature scale: the monoclinic form III(γ), the monoclinic form II(α), and the triclinic form I(β). Form II(α) is the one which is isomorphous with the solid form taken by BrCl, ClI, BrBr, and BrI. The transition temperatures and the heat effects of the transitions are shown in Table 5.2.

In the binary phase diagrams, measured for temperatures above room temperature, and with ClCl as the first component, ClCl's polymorphism gives rise to an almost negligible single-phase field for the form I(β). It means that, for the thermodynamic analysis of the phase diagrams, the existence of form I(β) can be ignored. However, for the analyses, the metastable melting properties of form II(α) are needed. The

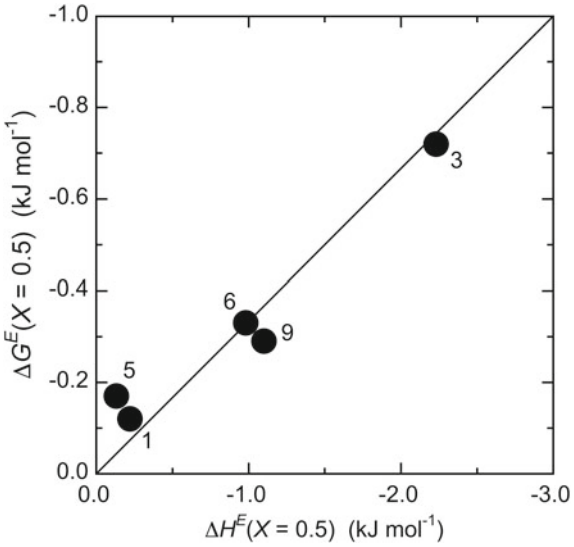

Fig. 5.1 *Para*-dihalobenzene family of systems. Excess Gibbs energy difference, $\Delta G^E(X = 0.5)$, as a function of the excess enthalpy difference, $\Delta H^E(X = 0.5)$, for systems with complete miscibility. The numbering is in line with Table 5.1 (reproduced from Ref. [3], © 1991, with permission from Elsevier)

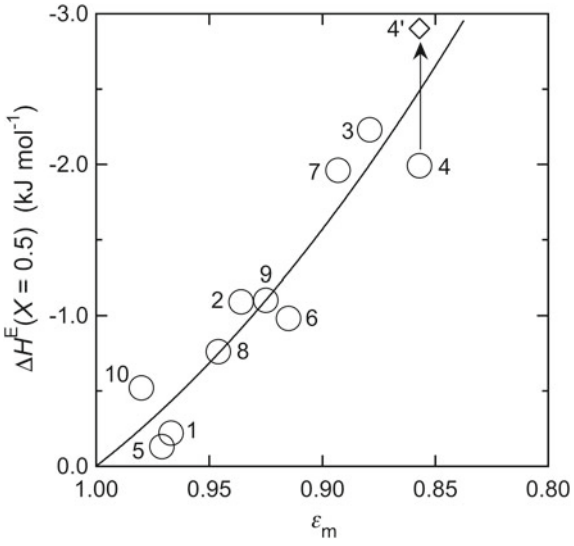

Fig. 5.2 *Para*-dihalobenzene family of systems. Excess enthalpy difference, $\Delta H^E(X = 0.5)$, as a function of the coefficient of crystalline isomorphism, ε_m. ○: data from Table 5.1; numbering in line with Table 5.1. ◊: improved value for system ClCl + BrI, taking into account the extension of the miscibility gap; see Sect. 5.3 (adapted from Ref. [3], © 1991, with permission from Elsevier)

Table 5.2 Temperatures and enthalpies of transition of *p*-dichlorobenzene as obtained by adiabatic calorimetry [1, 9]

Transition	T (K)	ΔH (J mol^{-1})
III(γ) → II(α)	275.0 ± 0.2	1238 ± 7
II(α) → I(β)	306 ± 1	181 ± 6
I(β) → liquid	326.24 ± 0.03	17,907 ± 15

metastable melting point (α–liquid) calculated from the data presented in Table 5.2 is 326.05 K; the heat of melting is 18,027 J mol^{-1} [8]. Oonk et al. [8] in their analysis of the system ClCl + BrI, used the calculated values of 326.03 K and 18,088 J mol^{-1}, respectively (based on the data by Dworkin et al. [10]). In that analysis, the extension of the miscibility gap was also taken into account, as a result of which the improved value of −2900 J mol^{-1} (see Fig. 5.2) was obtained for $\Delta H^E(X = 0.5)$. In addition, the three-phase equilibrium solid I + solid II + liquid was estimated at $T = 324$ K, along with $X(\text{I}) = 0.005$; $X(\text{II}) = 0.010$; $X(\text{liq}) = 0.049$.

5.4 The System *p*-Dichlorobenzene + *p*-Dibromobenzene

In 1938, Deffet [11] published a paper on the influence of high pressure on the melting curves of binary mixtures. The study included the system *p*-dichlorobenzene + *p*-dibromobenzene, which was investigated at atmospheric pressure and at pressures of about 500 and 1000 atm. The solidus and liquidus curves in Deffet's phase diagram, at atmospheric pressure, are in line with the results of the earlier investigations by Küster [12], Bruni and Gorni [13], Beck and Ebbinghaus [14], Beck [15], and Kruyt [16]. In Deffet's phase diagram, the distance between solidus and liquidus at equimolar composition is 9 K. For the determination of the solidus points (which, unlike liquidus points, are not clearly discernible on cooling/heating curves), Deffet employed the visual heating method discussed by Beck and Ebbinghaus [14].

In 1948, Campbell and Prodan [17] published the description of 'an apparatus for refined thermal analysis', along with the results obtained for the ternary system *p*-dichlorobenzene + *p*-dibromobenzene + *p*-bromochlorobenzene. In Fig. 5.3a, it is shown how Campbell and Prodan derived liquidus and solidus temperatures from their carefully obtained cooling curves.

As regards the binary subsystem *p*-dichlorobenzene + *p*-dibromobenzene, Campbell and Prodan's liquidus data are in agreement with the results of the earlier investigations; their solidus data, however, are not (at the equimolar composition the distance between solidus and liquidus is less than 5 K). In spite of all this, Campbell and Prodan's liquidus data are of unparalleled accuracy.

Next, Campbell and Prodan's liquidus data, along with the melting properties of the pure components, were used by van Genderen et al. to calculate the solidus of the system using LIQFIT. The calculated phase diagram is shown in Fig. 5.3b. In the phase

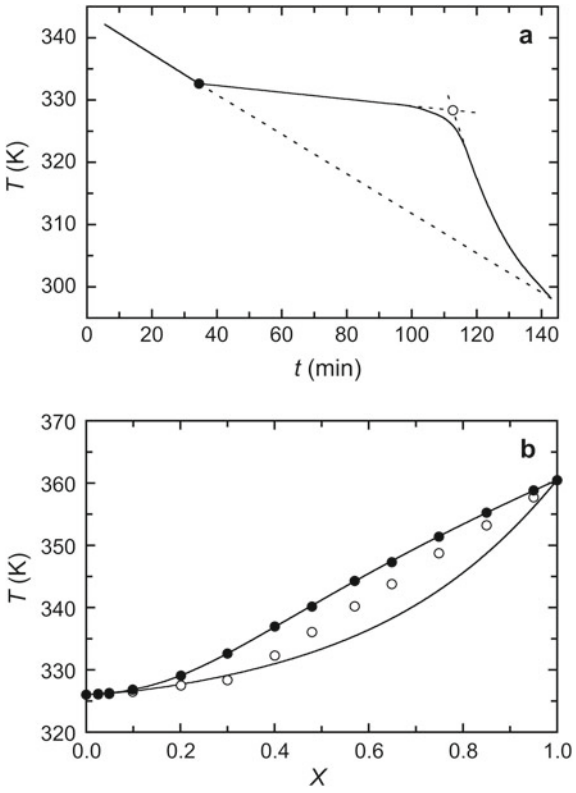

Fig. 5.3 System {(1 − *X*) *p*-dichlorobenzene + *X* *p*-dibromobenzene}. **a** Typical cooling curve obtained by Campbell and Prodan [17], showing how liquidus (●) and solidus (○) points were derived from it ($X = 0.3003$, $T_{liq} = 332.64$ K). **b** Phase diagram calculated by LIQFIT using Campbell and Prodan's liquidus data (●) [18] (**a** reproduced from Ref. [17], © 1948, with permission from American Chemical Society)

diagram obtained by LIQFIT, the distance between solidus and liquidus at equimolar composition is 8 K.

Apart from the thermodynamic phase diagram analysis, van Genderen et al. [18] studied, by DSC, the melting behaviour of samples prepared by *zone levelling*, employing the instrument designed by Kolkert [19, 20]. They found that the zone-levelled material is changing from solid to liquid in a quasi-isothermal manner, just like the pure components of the system; see Fig. 5.4. For comparison, the melting curve labelled 'c' (Fig. 5.4) is representative of an everyday DSC recording of mixed crystalline material prepared by melting and quenching in the instrument.

Most interestingly, the melting points of the levelled samples are situated on the *equal-G curve* of the calculated phase diagram; see Fig. 5.5. The equal-*G* curve (EGC) is the locus in the *TX* plane of the temperatures at which solid and liquid of the same composition have equal molar Gibbs energies (see Chap. 3). Surprisingly,

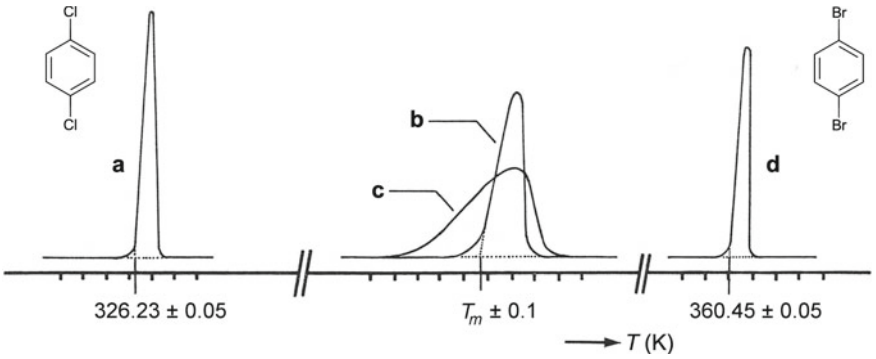

Fig. 5.4 System {(1 − *X*) *p*-dichlorobenzene + *X* *p*-dibromobenzene}. Typical melting curves measured with DSC with a heating rate of 0.62 K min^{-1} and a sample mass of 1 mg. **a** *p*-dichlorobenzene pure; **b** zone-levelled sample; **c** quenched sample; **d** *p*-dibromobenzene pure (reproduced from Ref. [18], © 1977, with permission from De Gruyter)

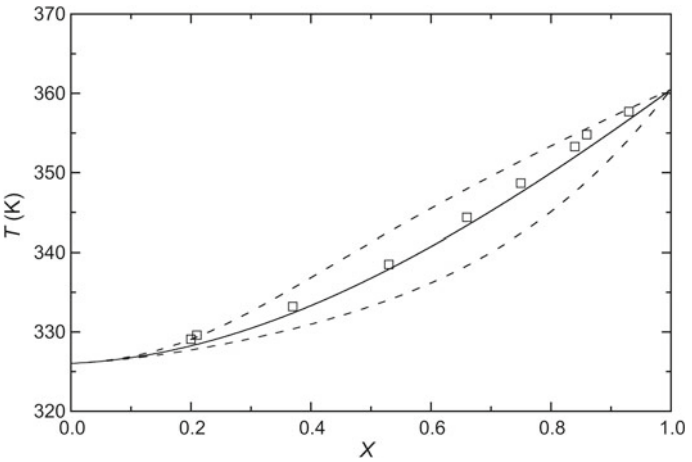

Fig. 5.5 System {(1 − *X*) *p*-dichlorobenzene + *X* *p*-dibromobenzene}. The 'melting points' of zone-levelled mixed crystals (□) registered by DSC, are situated on the equal-*G* curve (—). Dashed lines represent the solidus and liquidus calculated using LIQFIT (adapted from Ref. [18], © 1977, with permission from De Gruyter)

the EGC is more than an auxiliary curve in theoretical work — in that its course, like the course of the liquidus e.g., can be revealed by experimental methods.

It may be clear that the experimental determination of the equal-*G* curve is possible only if a number of severe conditions are simultaneously satisfied. These are, for the sample, compactness and a high degree of homogeneity, and for the experiment, the use of a high heating rate.

When studied by *adiabatic calorimetry*, mixed crystalline material prepared by zone levelling neatly starts to produce liquid at the temperature of the solidus, and

the material is fully liquid at the temperature of the liquidus. A beautiful example is shown in Fig. 5.6.

The experimental data in Fig. 5.6 (open circles) also show that quenching a liquid mixture does not yield a mixed crystalline material that is suitable for determination of reliable solidus temperatures. As can be seen in Fig. 5.7, the same holds for mixed crystalline material that is prepared by slow cooling (3 K per day) after annealing for five days at a temperature just below the liquidus temperature.

To circumvent the laborious task of zone levelling, van der Linde prepared mixed crystalline material by rapid evaporation of a volatile solvent, and, subsequently, studied the melting behaviour of the material by adiabatic calorimetry [1, 23]. A typical example from van der Linde's work is the *heat-capacity melting curve* (C_p–T graph) as shown in Fig. 5.8.

Van der Linde developed a method, referred to as *ULTRACAL*, with the help of which one can assess the heat-capacity melting curve of the kind shown in Fig. 5.8, and at the same time, establish the solidus and liquidus temperatures of the phase diagram. The method was tested on the system *p*-dichlorobenzene + *p*-dibromobenzene, and subsequently applied to the system 1,3,5-trichlorobenzene + 1,3,5-tribromobenzene; see Sect. 5.5.

For the system *p*-dichlorobenzene + *p*-dibromobenzene, mixed crystalline material prepared by rapid evaporation of a solvent was also used by Haget et al. in a DSC study [5]. The derived solidus and liquidus data were found to be, within experimental uncertainty, in full agreement with the calculated diagram as shown in Figs. 5.3b and 5.5 (see also van der Linde et al. [23]).

Overviewing the history of the system *p*-dichlorobenzene + *p*-dibromobenzene, it is surprising, and at the same time reassuring to know, that the DSC methodology, which is fast and uncomplicated, is capable of revealing not only the system's liquidus curve but also its solidus curve.

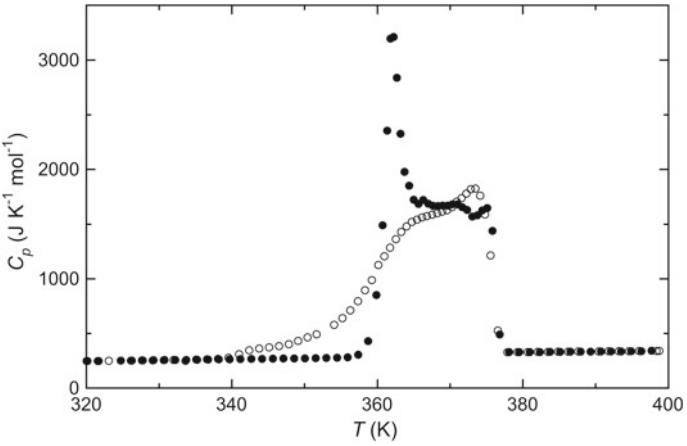

Fig. 5.6 System {(1 − X) *trans*-azobenzene + X *trans*-stilbene}. Heat-capacity melting curves (C_p–T graph) of a zone-levelled mixture (●) and a quenched mixture (○) having the same composition of $X = 0.503$ [21, 22] (reproduced from Ref. [22], © 1985, with permission from Elsevier)

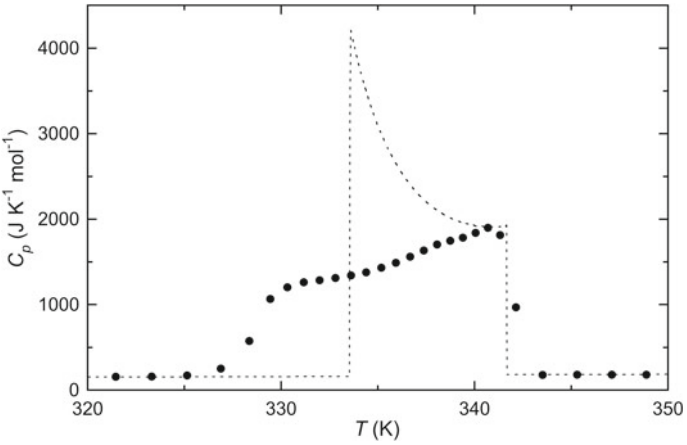

Fig. 5.7 System {(1 − X) *p*-dichlorobenzene + X *p*-dibromobenzene}. Heat-capacity melting curves of a mixture prepared by slow cooling (3 K per day) of the liquid; $X = 0.519$. ●: Experimental data; – – –: calculated ideal melting curve [1]

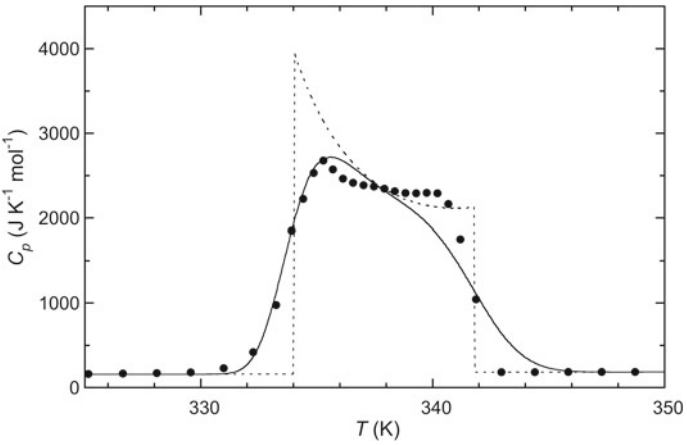

Fig. 5.8 System {(1 − X) *p*-dichlorobenzene + X *p*-dibromobenzene}. Heat-capacity melting curves of a mixture of prepared by rapid evaporation; $X = 0.515$ [1, 23]. ●: Experimental data; —: outcome of the simulation by ULTRACAL; – – –: calculated ideal melting curve (reproduced from Ref. [23], © 2002, with permission from Elsevier)

5.5 Tri- and Tetrasubstituted Halobenzenes

The binary systems 1,3,5-trichlorobenzene + 1,3,5-tribromobenzene and 1,2,4,5-tetrachlorobenzene + 1,2,4,5-tetrabromobenzene can be regarded as model systems in the study of the mixing properties and phase diagrams of 1,3,5-tri- and 1,2,4,5-tetrasubstituted halobenzenes.

The substances 1,3,5-trichlorobenzene and 1,3,5-tribromobenzene are isomorphous: orthorhombic, space group $P2_1P2_1P2_1$, with four molecules per unit cell. As a part of his thesis work, van der Linde [1, 23] showed on the basis of (i) direct measurement of the excess Gibbs energy of the mixed liquid phase ($G^{E,\mathrm{liq}}(X = 0.5) = 94$ J mol^{-1}) and (ii) an ULTRACAL analysis of four heat capacity melting curves that the system simply has a phase diagram of type [0], just like the systems 1, 2, 5, 8, and 10 of the *para*-dihalobenzenes (see Table 5.1), and the systems *trans*-azobenzene + *trans*-stilbene and thiophene + benzene (see Fig. 5.19).

The solid-liquid phase behaviour of the tetrasubstituted system, however, is much more complex than the behaviour of the trisubstituted system. In the case of the system 1,2,4,5-tetrachlorobenzene + 1,2,4,5-tetrabromobenzene, three solid forms make their appearance:

(i) the form α, which is the low-temperature form of the chloro compound;
(ii) the form β, which is the high-temperature form of the chloro compound, and at the same time, the low-temperature form of the bromo compound; and

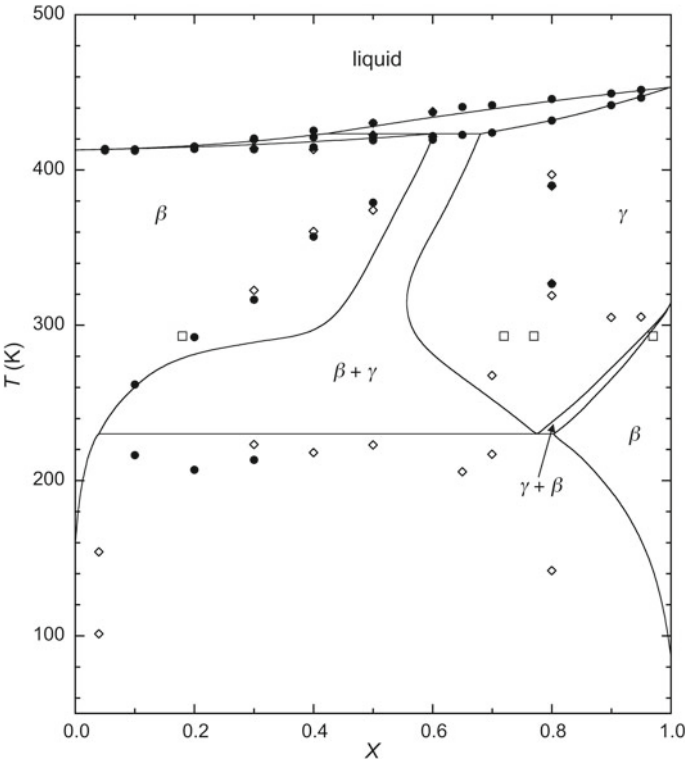

Fig. 5.9 Phase diagram of {$(1 - X)$ 1,2,4,5-tetrachlorobenzene + X 1,2,4,5-tetrabromobenzene}. Experimental data and calculated phase diagram assuming *crossed isodimorphism* between the two components. ●: DTA; □: XRD; ◊: Guinier-Lenné, Guinier-Simon [24]; —: calculated phase diagram [25] (reproduced from Ref. [25], © 1991, with permission from Elsevier)

(iii) the form γ, which is the high-temperature form of the bromo compound.

At room temperature, β is the stable form of the chloro as well as the bromo compound. Experimental data, X-ray diffraction and thermal analysis, are from Mondieig et al. [24].

An unorthodox thermodynamic assessment has been presented by van Genderen et al. [25]. It was assumed that the γ form of pure 1,2,4,5-tetrachlorobenzene is identical with the β form, thus circumventing the problem of determining the metastable γ–β transition temperature and transition entropy. Furthermore, the low-temperature α form was neglected. The outcome of the assessment is a model that yields a phase diagram that is in adequate agreement with the experimental data and accounts for the various phase fields. The result, along with the experimental data, is shown in Fig. 5.9.

5.6 The Family of the 2-Substituted Naphthalenes; the Existence of Two Subfamilies

Naphthalene and its 2-*R*-substituents, with R = F, Cl, Br, SH, CH_3, and OH, all crystallize, at temperatures near their melting point, in the space group $P2_1/a$. All have two molecules per unit cell, and for the derivatives this involves molecular disorder, in that, on a given lattice site, there are four possible orientations of the molecules [26]; see Fig. 5.10.

In spite of the fact that the seven substances have similar cell dimensions, there are two structural subfamilies, denoted by f_1 and f_2, with slightly different types of molecular arrangement. This circumstance was described by Kitaigorodsky [27] as '*all the naphthalene β-derivatives are supposed to possess similar energy surfaces which have two minima approximately of the same depth. One of them leads to the fluoronaphthalene packing, the second to the naphthalene type packing*'. Kitaigorodsky's view is reflected in Fig. 5.11.

A member of subfamily f_1, say 2-fluoronaphthalene, is not isomorphous with a member of subfamily f_2, say naphthalene. This implies that the two do not give rise to a continuous series of mixed crystals; see Fig. 5.12. The system naphthalene + 2-fluoronaphthalene is an example of crossed isodimorphism (see also Sect. 5.10).

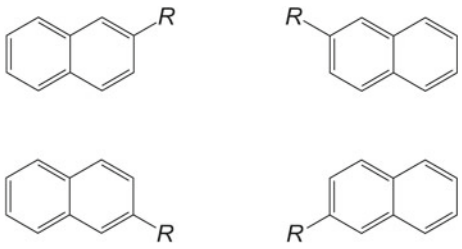

Fig. 5.10 Four orientations of the molecules of 2-substituted naphthalenes

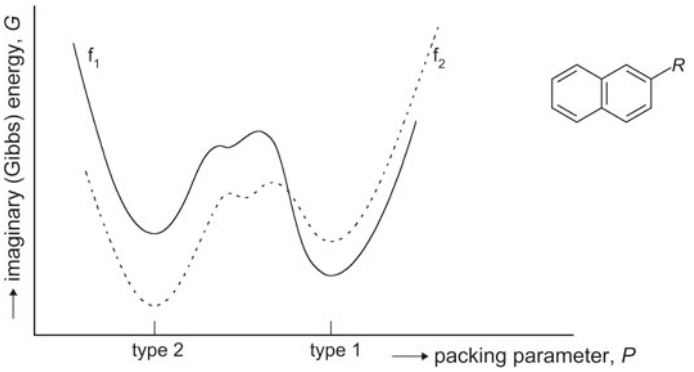

Fig. 5.11 2-Substituted naphthalenes. Imaginary (Gibbs) energy function G versus packing parameter P for the $P2_1/a$ unit cell with two molecules. —: f_1 subfamily with R = F, Cl, Br, SH and CH_3; – – –: f_2 subfamily with R = H (and OH). The stable form of naphthalene (R = H) is different from the stable form taken by the members of the f_1 subfamily [28, 29] (reproduced from Ref. [29], © 1991, with permission from EDP Sciences)

5.7 The System Naphthalene + 2-Naphthol

At the time of writing the paper on 2-substituted naphthalenes and the existence of two subfamilies (1991; Ref. [29]), there was some confusion about the status of the substance 2-naphthol (R = OH): f_1 or f_2? In a sense, the confusion is related to the fact that 2-naphthol's $P2_1/a$ form with two molecules per unit cell (α) has a stable existence of just 0.6 K; from T = 392.6 K to the melting point T = 393.2 K.

A key system, with 2-naphthol as one of the components, is naphthalene + 2-naphthol. The literature about this system has been reviewed by Oonk and Tamarit [31]; at this place, a short summary is given.

The experimental determination of the phase diagram goes back to 1895 and 1909 when Küster [32] determined liquidus temperatures and Rudolfi [33] determined both liquidus and solidus temperatures. The diagram published by Rudolfi has the cigar-type of solid–liquid loop, type [0], characteristic of complete subsolidus miscibility. The same type of diagram was published by Vetter et al. in 1963 [34]. Vetter's work is unique in that, by means of a technique related to *zone melting*, the true equilibrium compositions of the solid and liquid phases in equilibrium had been determined. The system was used as an example in a paper on the derivation of *distribution coefficients* from phase diagrams by Oonk and Pleijsier [35] who demonstrated the agreement between the calculated phase diagram and Vetter's experimental data. Kolkert [19, 20] used the system to demonstrate the performance of his zone-levelling instrument for the growth of homogeneous mixed crystals (see also Sect. 5.4). After Baumgarth et al. [36], in 1969, had published their phase diagram, including the solid–solid two-phase region, a number of conflicting diagrams were published [37–40] until in 1998 Michaud et al. [41], by careful experimentation, confirmed the basic structure of the diagram by Baumgarth et al. [36]; see Fig. 5.13. The substance 2-naphthol, as a result, unmistakably is a member of the subgroup f_2.

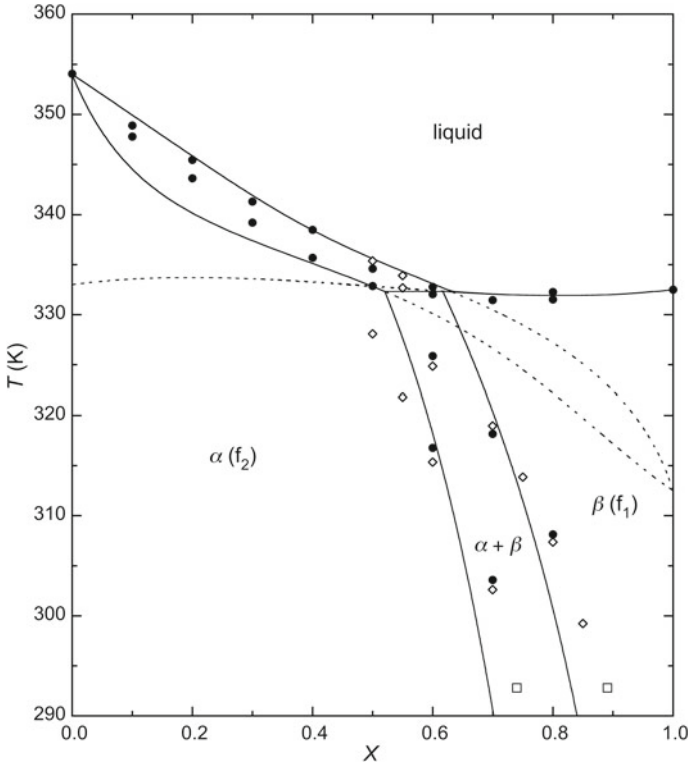

Fig. 5.12 Phase diagram of $\{(1 - X)$ naphthalene $+ X$ 2-fluoronaphthalene$\}$. Experimental points and calculated phase diagram assuming crossed isodimorphism. ●: DTA/DSC; □: XRD; ◊: Guinier-Lenné [40]; —: calculated phase diagram; – – –: calculated metastable parts of the solid–liquid equilibrium curves [30] (reproduced from Ref. [30], © 1989, with permission from Elsevier)

Another system, found by Rudolfi [33] to show complete subsolidus miscibility — phase diagram with a minimum, type [–] — is the combination of naphthalene and 2-aminonaphthalene. Accordingly, 2-aminonaphthalene would be the third member of the subgroup f_2.

5.8 The Halo + Halo Systems

The 2-halonaphthalenes (halo = F, Cl, Br) belong to the subfamily f_1. The same holds true for 2-thionaphthalene, whose properties are such that it can be taken here as a member of the group of the 2-halonaphthalenes. The four substances comprise six binary combinations, all of them showing complete subsolidus miscibility [40].

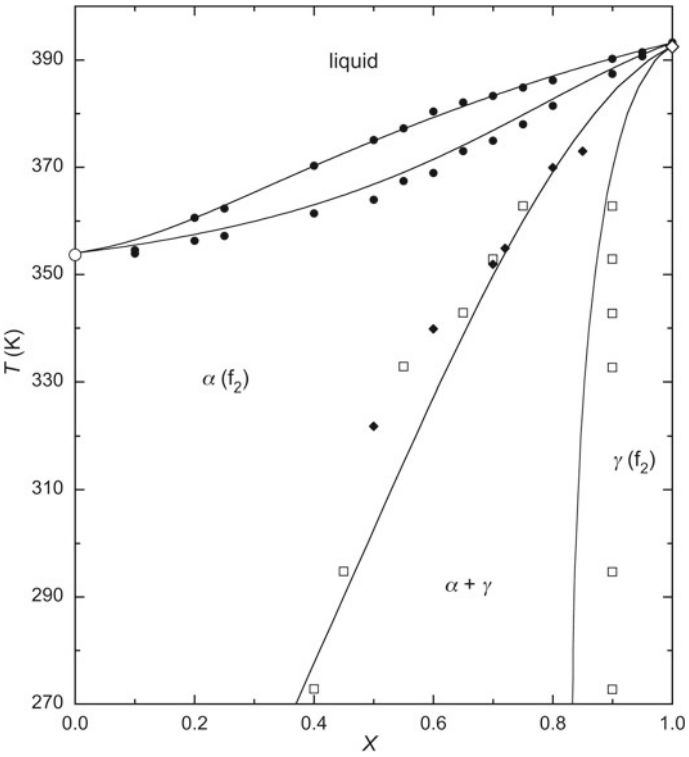

Fig. 5.13 Phase diagram of the system $\{(1 - X)$ naphthalene $+ X$ 2-naphthol$\}$. ●: DSC on heating; □: RT-XRD; ◆: Guinier-Simon heating analysis; ○: stable melting point of naphthalene (α–liquid); ◊: γ–α transition temperature of 2-naphthol; —: calculated phase diagram (reproduced from Ref. [41], © 1998, with permission from EDP Sciences)

Quite like the *para*-dihalobenzene systems (see Calvet et al. [3] and Fig. 5.2), the binary 2-halonaphthalene systems have mixing/excess properties whose magnitude increases with an increasing geometric mismatch (decreasing value of ε_m); see Fig. 5.14.

5.9 The Methyl + Halo Systems

The three methyl + halo 2-substituted naphthalene systems all have complete subsolidus miscibility; the phase diagrams for halo = Cl, Br have a maximum, type [+], which is quite exceptional, whereas methyl + F has a phase diagram of type [0]. The system methyl + SH also has a type [0] phase diagram [40].

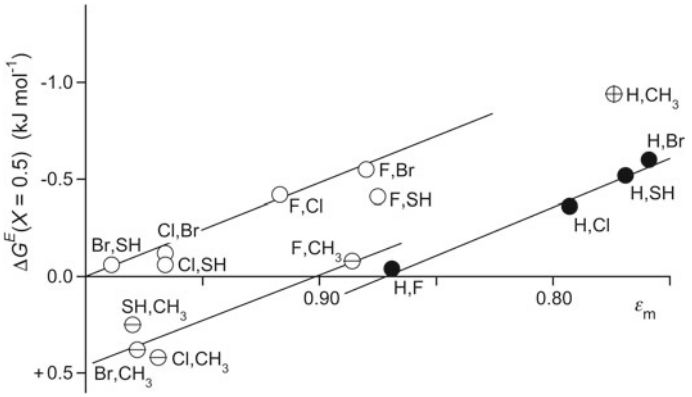

Fig. 5.14 Family of the 2-substituted naphthalenes. Equimolar excess Gibbs energy difference, $\Delta G^E(X = 0.5)$, as a function of the coefficient of crystalline isomorphism, ε_m (after Oonk et al. [29]). For numerical values of ε_m, see Haget et al. [26] (reproduced from Ref. [29], © 1991, with permission from EDP Sciences)

This time the components of the system not only differ as regards the size of their molecules but also as regards their *chemical nature*. As a result, the thermodynamic excess properties of the system have or may have, apart from a 'geometric contribution', also a 'chemical contribution'.

In the case of the methyl + halo systems there is, indeed, a chemical contribution, as can be inferred from Fig. 5.14. In terms of ΔG^E, the chemical contribution at equimolar composition has a value of about +0.5 kJ mol^{-1} (in Fig. 5.14 given by the intersection with the vertical axis, where the contribution of geometric mismatch is zero; $\varepsilon_m = 1$). Ignoring any excess behaviour of the liquid mixtures, the positive ΔG^E represents a negative excess Gibbs energy of the mixed crystalline state, read, an extra attraction between halo and methyl (geometric mismatch, on the other hand, corresponds to an extra effect of a repulsive nature). Note that in the case of the methyl + fluoro system the geometric and the chemical contribution virtually compensate one another.

A detailed analysis of the methyl + halo systems has been presented by Calvet et al. [42], whose study includes a computer search on the statistics of *intermolecular contacts* in pure substances containing methyl and halogen — to find out in which way the extra attraction is reflected by radial frequency distributions $f(R)$:

$$f(R) = \frac{N(R)}{(4 \cdot \pi \cdot R^2 \cdot \Delta R) \cdot N_T} \tag{5.6}$$

in which R represents the distance between the atoms and N the number of contacts. The property $f(R)$ 'corrects', for a given contact such as F–CH$_3$, $N(R)$ — in fact the number of contacts between $(R - 0.5 \cdot \Delta R)$ and $(R + 0.5 \cdot \Delta R)$ — for the geometrical factor $4\pi \cdot R^2 \cdot \Delta R$ and for the total number of contacts, N_T, for which $R < 10$ Å. The class width of the distribution, ΔR, had been set at 0.2 or 0.4 Å. It

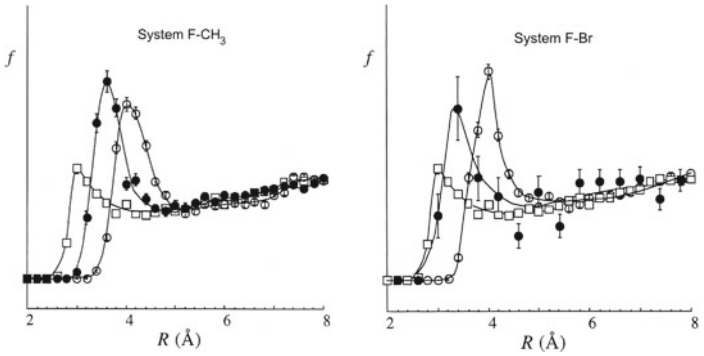

Fig. 5.15 Radial frequency distributions $f(R)$ in 2-substituted naphthalenes. Left graph: between F and CH_3 (●), F and F (□), CH_3 and CH_3 (○); right graph: between F and Br (●), F and F (□), Br and Br (○) (reproduced from Ref. [42], © 1999, with permission from AIP Publishing)

was found, among other things, that the peak of the distribution of F–Br contacts is more or less the average of F–F and Br–Br; and that, for F–CH_3, on the other hand, the peak for F–CH_3 is considerably higher than each of the two peaks F–F and CH_3–CH_3; see Fig 5.15.

The attractive nature of the combination substituted methyl and halogen, expressed by a phase diagram with a maximum, is also found in the system 1-methyl-2,3,5-tribromobenzene + 1-methyl-2,4,6-tribromobenzene; see Fig. 5.16, system 5. The experimental data, on which Fig. 5.16 is based, were collected by Jaeger in 1904 [43]; a thermodynamic analysis was made by Oonk [44]. 1-Methyl-2,3,5-tribromobenzene and 1-methyl-2,4,6-tribromobenzene (components II and V in F. M. Jaeger's classification of tribromotoluene binary systems) show the same crystal system with the same characteristics.

NB. A theoretical underpinning of any extra attractive effect between methyl and halogen is lacking. Computations using modern methods of theoretical chemistry — on the combination –CH_3 and –Cl — failed to reveal the 'desired' effect [45].

5.10 Crossed Isodimorphism

In terms of chemically coherent groups, naphthalene is not a substance like the 2-halonaphthalenes. Neither, the 2-halonaphthalenes, which all belong to the f_1 group, are isomorphous with naphthalene, which is a member of the f_2 group. As a consequence, complete subsolidus miscibility for a naphthalene + 2-halonaphthalene system is out of the question. The stable solid–liquid phase diagram will show a three-phase equilibrium situation where three two-phase branches come together, such as is seen in Fig. 5.12, for the combination of naphthalene and 2-fluoronaphthalene, and with the phase symbols α for f_2 and β for f_1. The system is a case of crossed isodimorphism (see also Chap. 4): the stable phase diagram is the result of two,

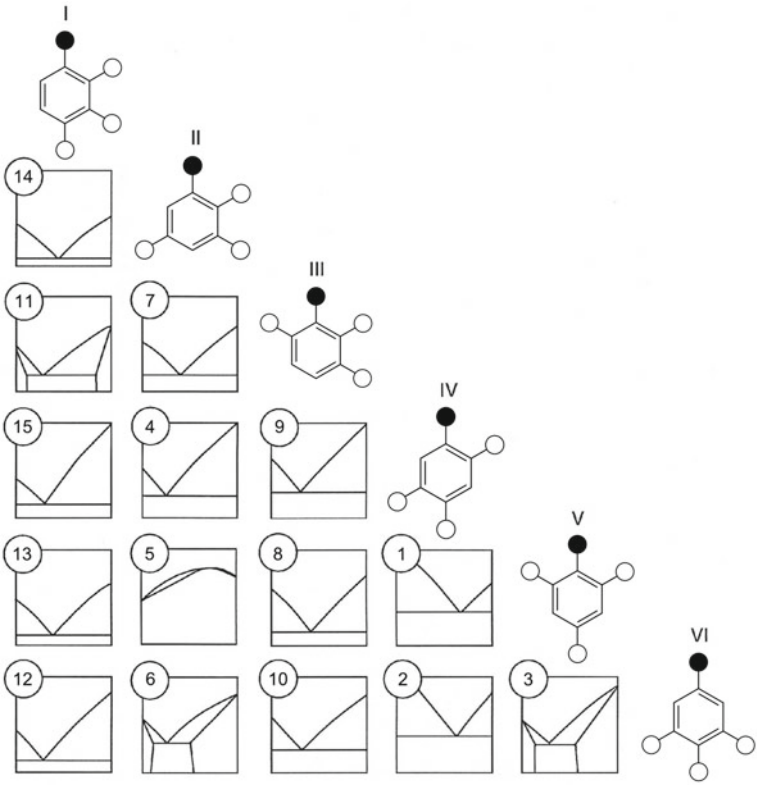

Fig. 5.16 F. M. Jaeger's classification of the 15 tribromotoluene binary systems [43]. ●: CH_3; ○: Br (reproduced from Ref. [44], © 1992, with permission from Elsevier)

each other crossing solid–liquid loops. Each of these two loops emanates from a *stable melting point* and ends in a metastable melting point. The assessment of the metastable melting points is an essential part of the thermodynamic analysis of such a system.

The thermodynamic analysis, presented by van Duijneveldt et al. [30], comprises the five systems naphthalene + 2-*R*-naphthalene with R = F, Cl, Br, SH, CH_3. The outcome of van Duijneveldt's analysis, as regards the equimolar ΔG^E involving the f_1 mixed solid, is included in Fig. 5.14, from which it follows that the naphthalene + 2-halonaphthalene systems line up with the 2-methylnaphthalene + 2-halonaphthalene systems. The outcome for the naphthalene + 2-methylnaphthalene system is more or less in line with the halo + halo systems, of which the mixing effects come from geometric mismatch.

Besides, instructive examples of thermodynamic phase diagram analysis in the case of crossed isodimorphism are the ones applied to the system naphthalene + 2-fluoronaphthalene (see Fig. 5.12) and the system thianaphthene + naphthalene (see Fig. 5.20).

5.11 The System *trans*-Azobenzene + *trans*-Stilbene

The text presented here for the system *trans*-azobenzene + *trans*-stilbene is inspired by the thesis work of Bouwstra [21, 22, 46–50]. Special attention is given to the outcome of *lattice energy* calculations, because this part of Bouwstra's work can only be found in her thesis.[2]

The substances *trans*-azobenzene and *trans*-stilbene, see Fig. 5.17, are isomorphous and give mixed crystals in all proportions. Their space group is $P2_1/c$ with four molecules per unit cell on two independent sites, referred to as site A and site B. On site B, there is *orientational disorder*, such that there are two distinct orientations of the molecules; on site A, this kind of disorder is absent; see Fig. 5.18, for the case of *trans*-stilbene.

In the mixed crystals of the two substances, there is a complex interplay of *substitutional disorder*, due to the interchange of *trans*-azobenzene and *trans*-stilbene, and the orientational disorder on site B.

To give an idea of how the sites are occupied, as derived from X-ray structure refinement, the case is taken of a part of a mixed crystal, which has 740 molecules of *trans*-azobenzene and 260 molecules of *trans*-stilbene ($X = 0.26$). On site B, there are 318 azobenzene molecules and 182 stilbene molecules. Out of the 182 stilbene molecules, 160 have orientation B1 and 22 orientation B2 (and out of the 318 azobenzene molecules, 264 have the orientation B3 and 54 the orientation B4). On site A, there are 422 azobenzene and 78 stilbene molecules. These numbers show that the fraction α of *trans*-stilbene molecules that are on site A is equal to $78/(78 + 182) = 0.30$. For mixed crystals of composition $X = 0.56$, the fraction α is found as $\alpha = 0.39$.

The important thing to note is that the values of the parameter α, found by X-ray structure refinement, are beautifully reproduced by the computations of the lattice free energy ($\approx$ Gibbs energy). For $X = 0.26$, the lowest free energy is obtained for value $\alpha = 0.33$; and for $X = 0.56$, the lowest free energy was found for $\alpha = 0.40$.

In Table 5.3, the enthalpies of sublimation of *trans*-azobenzene and *trans*-stilbene and two mixed crystals are given. The values under the heading 'experimental' follow from vapour pressures as a function of temperature [48]. The enthalpy of sublimation values in the third column were obtained by calculation of the lattice energies, using the formalism and the data set constructed by Govers [53, 54]. The enthalpies of sublimation allow one to calculate the excess enthalpies of the mixed crystals; their values are given in the fourth column.

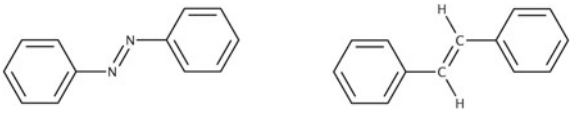

Fig. 5.17 Chemical structures of *trans*-azobenzene (left) and *trans*-stilbene (right)

[2] Although not discussed in this chapter, lattice energy calculations for *para*-dihalobenzenes have been presented by Oonk et al. [51] and van Eijck [52].

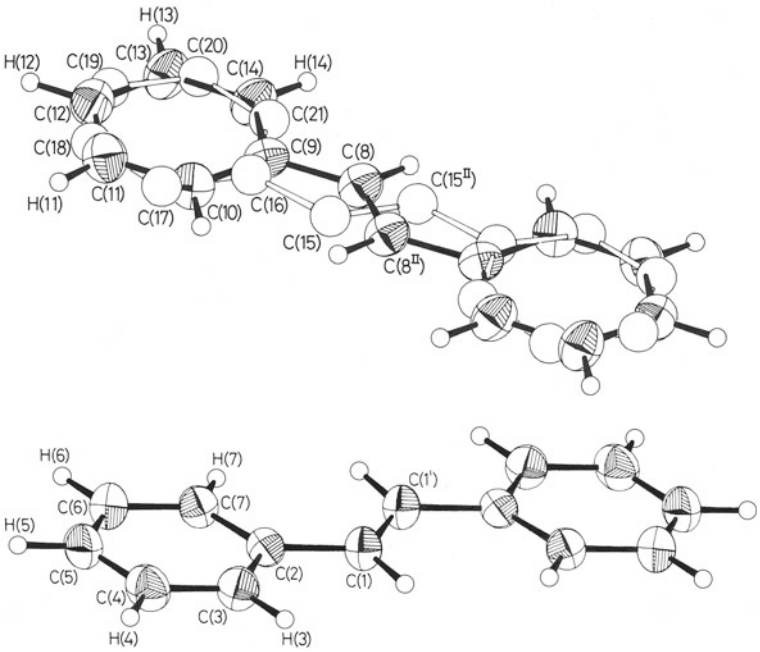

Fig. 5.18 *Trans*-stilbene. Top: a composite view of the disordered molecules at site B with 50% probability plots of thermal ellipsoids of the molecule with main-site occupancy in the disordered position (B1). Bottom: view of the molecule at site A with 50% probability plots of thermal ellipsoids [21, 47] (reproduced from Ref. [47], © 1984, with permission of the International Union of Crystallography)

Table 5.3 Enthalpies of sublimation, $\Delta_s^g H(298.15\ \mathrm{K})$, of *trans*-azobenzene and *trans*-stilbene and two mixed crystals: experimental data by Bouwstra et al. [48]; calculated data by Govers [53, 54], along with calculated excess enthalpy of the mixed solid phase ($H^{E,\mathrm{sol}}$)

	Experimental	Lattice energy calculation	
	$\Delta_s^g H_{\mathrm{exp}}$ (kJ mol^{-1})	$\Delta_s^g H_{\mathrm{calc}}$ (kJ mol^{-1})	$H^{E,\mathrm{sol}}$ (kJ mol^{-1})
Trans-azobenzene	94.65	96.1	0
$X = 0.26$		95.8	0.85
$X = 0.56$		96.5	0.78
Trans-stilbene	99.90	98.2	0

The two numerical values for the excess enthalpy in the fourth column of Table 5.3 allow one to calculate the two 'unknowns' A and B in Eq. (5.3). The calculated values are $A = 3400$ J mol^{-1} and $B = 0.6$.

In Fig. 5.19, upper graph, the solid–liquid phase diagram of the system *trans*-azobenzene + *trans*-stilbene is shown. Bouwstra et al. [22] used adiabatic calorimetry to obtain the experimental solidus points (open circles) and liquidus points (filled

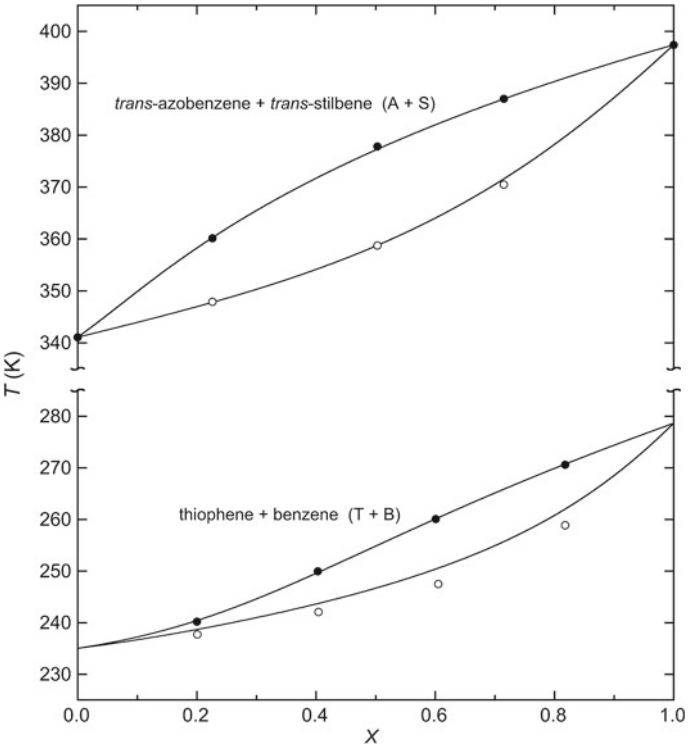

Fig. 5.19 Phase diagrams of the systems $\{(1 - X)$ *trans*-azobenzene $+ X$ *trans*-stilbene$\}$ (upper graph) and $\{(1 - X)$ thiophene $+ X$ benzene$\}$ (lower graph). ○: Experimental solidus points; ●: experimental liquidus points; —: calculated phase diagrams using LIQFIT. All experimental data were obtained by adiabatic calorimetry; samples of *trans*-azobenzene + *trans*-stilbene were prepared by zone levelling [22]; samples of thiophene + benzene were prepared by annealing [2, 55]

circles); see also Fig. 5.6. The liquidus points were subjected to a LIQFIT analysis, using the thermodynamic melting properties as obtained by Bouwstra et al. [22] and assuming ideal liquid mixtures. The outcome of the analysis is twofold: first the optimized phase diagram, and second the excess Gibbs energy of the solid state.

The optimized phase diagram is represented by the solidus and liquidus curves in Fig. 5.19 (upper graph). As can be seen, the calculated solidus is in excellent agreement with the experimental solidus points, thus, giving evidence for the high degree of homogeneity of mixed crystalline material that can be obtained by zone levelling.

The excess Gibbs energy, valid for the mean temperature of the diagram which is $T_m = 370$ K, is given by the expression

$$G^{E,\mathrm{sol}}(T = T_m, X) = 530 \cdot X \cdot (1 - X) \cdot [1 + 0.7 \cdot (1 - 2 \cdot X)]\,\mathrm{J\,mol^{-1}}. \quad (5.7)$$

In terms of Eqs. (5.2) and (5.3), the compensation temperature Θ follows from the equality: $530 = 3400 \cdot (1 - 370\ \mathrm{K}/\Theta)$; the result is $\Theta = 438$ K.

5.12 The System Thiophene + Benzene

Another system, whose change, from mixed crystalline solid to liquid, has been studied by adiabatic calorimetry, is the combination of thiophene and benzene: $C_4H_4S + C_6H_6$. Details of the investigation can be found in the papers by Okamoto et al. [55, 56] and Yamamuro et al. [2].

It is instructive to make a comparison between the systems thiophene + benzene (T + B) and *trans*-azobenzene + *trans*-stilbene (A + S), and so from the point of view of phenomenology and methodology.

The two systems have in common that they form mixed crystals in all proportions, and that their change from solid to liquid goes together with a cigar type of phase diagram (type [0]; see Fig. 5.19). In the (A + S) case, the formation of mixed crystals is facilitated by the high degree of molecular homeomorphism. In the case of (T + B), mixed crystals are easily formed due to the high degree of *rotational disorder*; caused by the pseudo-fivefold symmetry and the sixfold symmetry of the molecules of T and B, respectively.

The high degree of rotational disorder, which is most pronounced for thiophene, is reflected by the heats of melting: 5.0 kJ mol^{-1} for thiophene [57] and 9.9 kJ mol^{-1} for benzene [58], whereas the heats of melting of *trans*-azobenzene and *trans*-stilbene are 22.53 and 27.69 kJ mol^{-1}, respectively [22].

Another aspect of the rotational disorder is that homogeneous mixed crystals of (T + B) are easily formed. The mixed crystalline materials used in determining the solidus and liquidus temperatures as shown in Fig. 5.19 (lower graph) were obtained by annealing at a temperature just below the solidus point for 2–7 days. As can be seen, this relatively simple preparation method yields reasonable (although not superb) solidus temperatures for this system. In the case of (A + S), homogeneous mixed crystals had to be prepared by the laborious technique of zone levelling. As already mentioned, and shown in Fig. 5.19 (upper graph), this technique yields the best possible result.

5.13 The System Thianaphthene + Naphthalene

The binary system thianaphthene + naphthalene is another example of a system showing crossed isodimorphism. Although the molecules of thianaphthene (benzo[b]thiophene, C_8H_6S) and naphthalene are similar in shape and form, the substances crystallize in different crystal systems: thianaphthene is orthorhombic (β); naphthalene is monoclinic (α). This gives rise to an interrupted series of mixed

crystals. The solid–liquid phase diagram can be considered as the result of two interfering solid–liquid loops.

The phase diagram presented in Fig. 5.20 is the result of an extensive thermodynamic analysis [59, 60] of the available experimental data by Klipp et al. [59], Mastrangelo and Dornte [61], and Kravchenko and Pastukhova [62]. The metastable melting points ($\alpha \rightarrow$ liquid of thianaphthene, and $\beta \rightarrow$ liquid of naphthalene) and the corresponding transition enthalpies were derived by extrapolation of the available calorimetric data. For the α form of the system, the compensation temperature Θ in Eq. (5.2) was calculated as $\Theta = 420$ K.

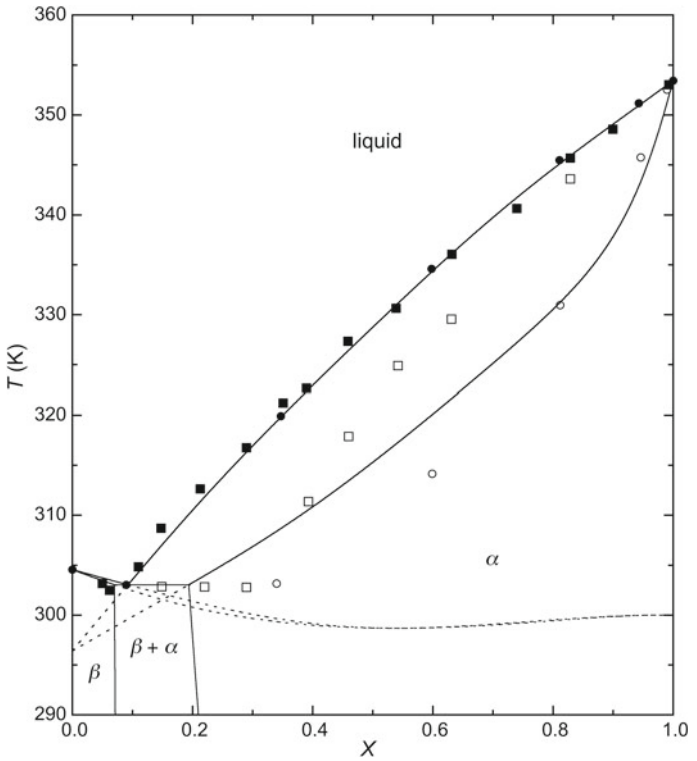

Fig. 5.20 Phase diagram of the system $\{(1 - X)$ thianaphthene $+ X$ naphthalene$\}$. ●, ○: Experimental liquidus and solidus data by Mastrangelo and Dornte [61]; ■, □: experimental liquidus and solidus data by Kravchenko and Pastukhova [62]; —: calculated phase diagram; – – –: calculated metastable extensions (reproduced from Ref. [60], © 1995, with permission from Springer)

5.14 Ternary Systems, as an Extra

As already mentioned in Sect. 5.4, the change from liquid to solid in the ternary system *p*-dichlorobenzene + *p*-dibromobenzene + *p*-bromochlorobenzene was studied by Campbell and Prodan [17].

In 1983, Moerkens et al. [63] published the results of an investigation in which the ternary liquidus and solidus surfaces had been calculated, starting from the thermodynamic melting properties of the pure components and the thermodynamic mixing properties of the three binary subsystems; see Fig. 5.21 for a typical result [7, 63]. It was found that the mean absolute difference between *calculated* liquidus temperatures and corresponding *experimental* liquidus temperatures, measured by Campbell and Prodan and taken for 39 points inside the composition triangle, was as little as 0.125 K!

Another investigation on a ternary system of isomorphic aromatic compounds was carried out by Teunissen, who studied the combination of *p*-dibromobenzene,

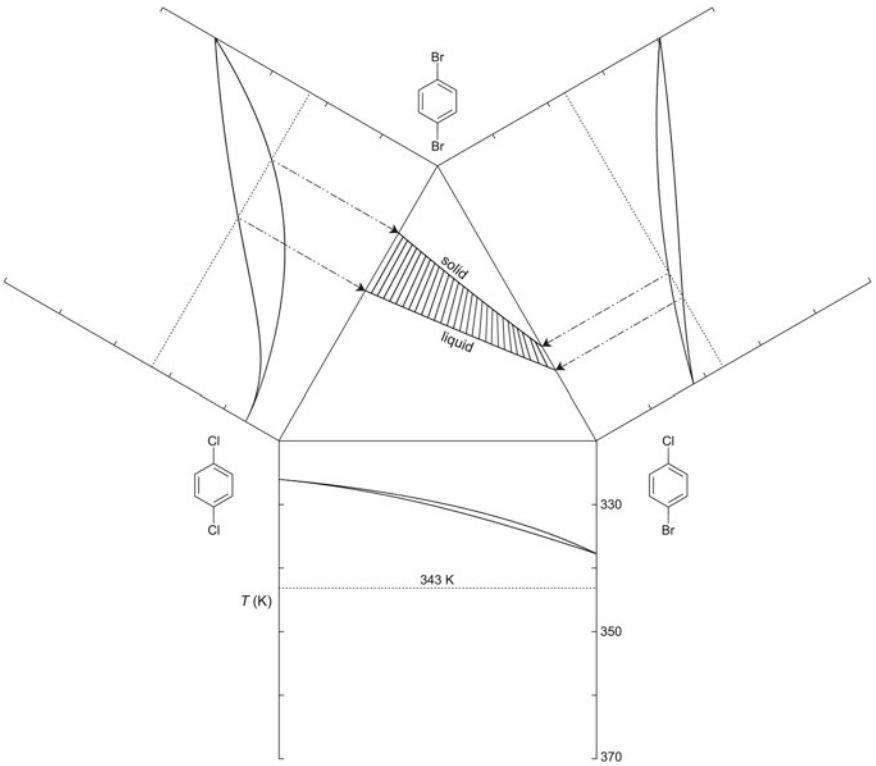

Fig. 5.21 Ternary solid–liquid phase diagram of the system *p*-dichlorobenzene + *p*-dibromobenzene + *p*-bromochlorobenzene at 343 K (adapted from Ref. [7], © 2008, with permission from Springer)

p-chloroiodobenzene, and *p*-bromoiodobenzene; see Oonk et al. [64]. Also worth mentioning is the study by Stolk et al. [65] on the ternary *n*-alkane system *n*-pentadecane + *n*-hexadecane + *n*-heptadecane.

References

1. Van der Linde PR (1992) Molecular mixed crystals from a thermodynamic point of view. Thesis, Utrecht University
2. Yamamuro O, Suga H, Usui Y, Kimura T, Takagi S (1997) Thermodynamic functions of the thiophene-benzene system in their liquid and solid solutions. J Phys Chem B 101:6541–6548
3. Calvet MT, Cuevas-Diarte MA, Haget Y, van der Linde PR, Oonk HAJ (1991) Binary *p*-dihalobenzene systems – correlation of thermochemical and phase-diagram data. Calphad 15:225–234
4. Bouwstra JA, Brouwer N, van Genderen ACG, Oonk HAJ (1980) A thermodynamic method for the derivation of the solidus and liquidus curves from a set of experimental liquidus points. Thermochim Acta 38:97–107
5. Haget Y, Housty JR, Maiga A, Bonpunt L, Chanh NB, Cuevas M, Estop E (1984) Alliages moléculaires à forte chaleur latente: système paradichlorobenzène (pDCB)-paradibromobenzène (pDBB). J Chim Phys 81:197–206
6. Cuevas-Diarte MA, Calvet T, Labrador M, Estop E, Oonk HAJ, Bonpunt L, Haget Y (1991) Coefficients of molecular homeomorphism and crystalline isomorphism in the series of para-disubstituted benzene derivatives. J Chim Phys 88:509–514
7. Oonk HAJ, Calvet MT (2008) Equilibrium between phases of matter, phenomenology and thermodynamics. Springer, Dordrecht
8. Oonk HAJ, Calvet T, Cuevas-Diarte MA, Tauler E, Labrador M, Haget Y (1995) Molecular alloys in the series of *para*-disubstituted benzene derivatives. Part 8. The *para*-dichlorobenzene + *para*-bromoiodobenzene system. Thermochim Acta 250:13–18
9. Van der Linde PR, van Miltenburg JC, van den Berg GJK, Oonk HAJ (2005) Low-temperature heat capacities and derived thermodynamic functions of 1,4-dichlorobenzene, 1,4-dibromobenzene, 1,3,5-trichlorobenzene, and 1,3,5-tribromobenzene. J Chem Eng Data 50:164–172
10. Dworkin A, Figuière P, Ghelfenstein M, Szwarc H (1976) Heat capacities, enthalpies of transition, and thermodynamic properties of the three solid phases of *p*-dichlorobenzene from 20 to 330 K. J Chem Thermodyn 8:835–844
11. Deffet L (1938) Recherches piézométriques. IV. Influences des hautes pressions sur la courbe de fusion des mélanges binaries. Bull Soc Chim Belg 47:461–505
12. Küster FW (1895) Beitrage zur Molekulargewichtsbestimmung an „festen Lösungen". 3. Mitteilung: Die isomorphen Mischungen von p-Dichlorbenzol mit p-Dibrombenzol und von s-Trichlorphenol mit s-Tribromphenol. Z Phys Chem 50U:65–80
13. Bruni G, Gorni F (1900) Sui fenomeni di equilibrio fisico nelle miscele de sostanze isomorfe. Gazz Chim Ital 30:127–140
14. Beck K, Ebbinghaus K (1906) Ueber Umwandlungspunkte und eine Methode zur Beobachtung derselben. Ber Dtsch Chem Ges 39:3870–3877
15. Beck K (1907) Beiträge zur relativen innern Reibung. Z Phys Chem 58:425–441
16. Kruyt HR (1912) Das Gleichgewicht Fest-Flüssig-Gas in binären Mischkristallsystemen. Z Phys Chem 79U:657–676
17. Campbell AN, Prodan LA (1948) An apparatus for refined thermal analysis exemplified by a study of the system *p*-dichlorobenzene–*p*-dibromobenzene–*p*-chlorobromobenzene. J Am Chem Soc 70:553–561

18. Van Genderen ACG, de Kruif CG, Oonk HAJ (1977) Properties of mixed crystalline organic material prepared by zone leveling. I. Experimental determination of the EGC for the system *p*-dichlorobenzene + *p*-dibromobenzene. Z Phys Chem (N F) 107:167–173
19. Kolkert WJ (1974) Growth of homogeneous organic mixed crystals by repeated pass zone levelling. Thesis, Utrecht University
20. Kolkert WJ (1975) Growth of uniform solid solutions of naphthalene and 2-naphthol by repeated pass zone-leveling. J Cryst Growth 30:213–219
21. Bouwstra JA (1985) Thermodynamic and structural investigations of binary systems. Thesis, Utrecht University
22. Bouwstra JA, de Leeuw VV, van Miltenburg JC (1985) Properties of mixed-crystalline organic material prepared by zone levelling. IV. Melting properties and excess enthalpies of (*trans*-azobenzene + *trans*-stilbene). J Chem Thermodyn 17:685–695
23. Van der Linde PR, Bolech M, den Besten R, Verdonk ML, van Miltenburg JC, Oonk HAJ (2002) Melting behaviour of molecular mixed crystalline materials: measurement with adiabatic calorimetry and modelling using ULTRACAL. J Chem Thermodyn 34:613–629
24. Mondieig D, Housty JR, Haget Y, Cuevas-Diarte MA, Oonk HAJ (1991) The system 1,2,4,5-tetrachlorobenzene + 1,2,4,5-tetrabromobenzene. Part 1. Experimental phase diagram (93–460 K). Thermochim Acta 177:169–186
25. Van Genderen MJ, Mondieig D, Haget Y, Cuevas-Diarte MA, Oonk HAJ (1992) A special model of isodimorphism used for the thermodynamic description of the system 1,2,4,5-tetrachlorobenzene + 1,2,4,5-tetrabromobenzene. Calphad 16:1–12
26. Haget Y, Bonpunt L, Michaud F, Negrier P, Cuevas-Diarte MA, Oonk HAJ (1990) Coefficients of molecular homeomorphism and crystalline isomorphism in the series of 2-*R*-naphthalene (*R* = H, F, Cl, CH_3, SH, Br). J Appl Crystallogr 23:492–496
27. Kitaigorodsky AI (1984) Mixed crystals. Springer-Verlag, Berlin-Heidelberg
28. Haget Y, Chanh NB, Meresse A, Bonpunt L, Michaud F, Negrier P, Cuevas-Diarte MA, Oonk HAJ (1999) Isomorphism and mixed crystals in 2-*R*-naphthalenes: evidence of structural subfamilies and prediction of metastable forms. J Appl Crystallogr 32:481–488
29. Oonk HAJ, van der Linde PR, Haget Y, Bonpunt L, Chanh NB, Cuevas-Diarte MA (1991) Molecular mixed crystals from a macroscopic thermodynamic point of view. J Chim Phys 88:329–341
30. Van Duijneveldt JS, Chanh NB, Oonk HAJ (1989) Binary mixtures of naphthalene and five of its 2-derivatives. Thermodynamic analysis of solid-liquid phase diagrams. Calphad 13:83–88
31. Oonk HAJ, Tamarit JLI (2005) Condensed phases of organic materials: solid-liquid and solid-solid equilibrium. In: Weir RD, De Loos ThW (eds) Measurement of the thermodynamic properties of multiple phases. Experimental thermodynamics, vol VII. Elsevier, Amsterdam
32. Küster FW (1895) Beitrage zur Molekulargewichtsbestimmung an „festen Lösungen". 2. Mitteilung: Das Gleichgewicht zwischen Wasser, Naphtalin und β-Naphtol. Z Phys Chem 17U:357–373
33. Rudolfi E (1909) Über die Dielektrizitätskonstanten von Gemischen fester Körper. Z Phys Chem 66U:705–732
34. Vetter H, Rössler S, Schildknecht H (1963) Theorie des Zonenschmelzens. Ermittlung der Solidus- und Liquiduskurve von Schmelzdiagrammen organischer Zweistoffsysteme durch Mikro-Zonenschmelzen und Normales Erstarren. In: Schildknecht H (ed) Symposium über Zonenschmelzen und Kolonnenkristallisieren. Kernforschungsanstalt, Karlsruhe, pp 57–68
35. Oonk HAJ, Pleijsier HL (1971) The equilibrium distribution coefficient and its derivation from *TX* solid-liquid equilibrium diagrams. Sep Sci 6:685–697
36. Baumgarth F, Chanh NB, Gay R, Lascombe J, Le Calvé N (1969) Contribution à l'étude de la phase cristalline haute température du β-naphtol et des solutions solides β-naphtol/naphthalène. J Chim Phys 66:862–868
37. Robinson PM, Rossell HJ, Scott HG, Legge C (1970) Binary phase diagrams of some molecular compounds—II. Mol Cryst Liq Cryst 11:105–117
38. Robinson PM, Scott HG (1972) The naphthalene–β-naphthol system. Mol Cryst Liq Cryst 18:153–156

39. Haget Y, Chezeau N, Meresse A, Housty J, Chanh NB (1979) Syncristallisation organique avec peritexie. Cas du système binaire fluoro-2 naphtalene – naphtol-2. Mol Cryst Liq Cryst 55:109–118
40. Meresse A (1981) Implications du polymorphisme dans la formation des alliages moléculaires. Syncristallisation en série naphtalénique β substituée. Thesis, Université de Bordeaux I
41. Michaud F, Negrier P, Haget Y, Alcobé X, Cuevas-Diarte MA, Oonk HAJ (1998) Is 2-naphtol isomorphous with 2-fluoronaphthalene or with naphthalene? J Chim Phys 95:2199–2213
42. Calvet T, Cuevas-Diarte MA, Haget Y, Mondieig D, Kok IC, Verdonk ML, van Miltenburg JC, Oonk HAJ (1999) Isomorphism of 2-methylnaphthalene and 2-halonaphthalenes as a revealer of a special interaction between methyl and halogen. J Chem Phys 110:4841–4846
43. Jaeger FM (1904) Ueber molekulare und krystallographische Symmetrie von stellungsisomeren Benzolabkömmlingen. Z Kristallog 38:555–601
44. Oonk HAJ (1992) Solid-liquid equilibria in the fifteen binary systems shared by the six isomeric tribromotoluenes. Homage to F.M. Jaeger. Calphad 16:37–46
45. Van Duijneveldt FB (2002) Personal communication
46. Bouwstra JA, Schouten A, Kroon J (1983) Structural studies of the system *trans*-azobenzene/*trans*-stilbene. I. A reinvestigation of the disorder in the crystal structure of *trans*-azobenzene, $C_{12}H_{10}N_2$. Acta Crystallogr C 39:1121–1123
47. Bouwstra JA, Schouten A, Kroon J (1984) Structural studies of the system *trans*-azobenzene/*trans*-stilbene. II. A reinvestigation of the disorder in the crystal structure of *trans*-stilbene, $C_{14}H_{12}$. Acta Crystallogr C 40:428–431
48. Bouwstra JA, Oonk HAJ, Blok JG, de Kruif CG (1984) Properties of mixed crystalline organic material prepared by zone levelling III. Vapour pressures of (*trans*-azobenzene + *trans*-stilbene). J Chem Thermodyn 16:403–409
49. Van Miltenburg JC, Bouwstra JA (1984) Thermodynamic properties of *trans*-azobenzene and *trans*-stilbene. J Chem Thermodyn 16:61–65
50. Bouwstra JA, Schouten A, Kroon J, Helmboldt RB (1985) Structural studies of the system *trans*-azobenzene/*trans*-stilbene. III. The structure of three mixed crystals of *trans*-azobenzene/*trans*-stilbene; determinations by X-ray and neutron diffraction. Acta Crystallogr C 41:420–426
51. Oonk HAJ, van Genderen ACG, Blok JG, van der Linde PR (2000) Vapour pressures of crystalline and liquid 1,4-dibromo- and 1,4-dichlorobenzene; lattice energies of 1,4-dihalobenzenes. Phys Chem Chem Phys 2:5614–5618
52. Van Eijck BP (2002) Crystal structure predictions for disordered halobenzenes. Phys Chem Chem Phys 4:4789–4794
53. Govers HAJ (1974) Calculations of lattice energies of unary and binary molecular crystals. Thesis, Utrecht University
54. Govers HAJ (1977) A mean-field approximation for multicomponent solid solutions of molecular crystals with orientational and substitutional disorder. J Chem Phys 67:4199–4205
55. Okamoto N, Oguni M, Suga H (1990) Transition phenomena in the thiophene crystal. Thermochim Acta 169:133–149
56. Okamoto N, Oguni M, Suga H (1989) Calorimetric study of thiophene-benzene solutions (I). J Phys Chem Solids 50:1285–1295
57. Figuière P, Szwarc H, Oguni M, Suga H (1985) Calorimetric study of thiophene from 13 to 300 K. Emergence of two glassy crystalline states. J Chem Thermodyn 17:949–966
58. Domalski ES, Hearing ED (1996) Heat capacities and entropies of organic compounds in the condensed phase. Volume III. J Phys Chem Ref Data 25:1–525
59. Klipp N, van der Linde PR, Oonk HAJ (1991) The system thianaphthene + naphthalene. Solid-liquid equilibrium. A case of crossed isodimorphism. Calphad 15:235–242
60. Oonk HAJ (1995) The syncrystallization of thianaphthene and naphthalene—an exercise in thermodynamic phase diagram analysis. In: Van der Eerden JP, Bruinsma OSL (eds) Science and technology of crystal growth. Kluwer Academic Publishers, pp 27–38
61. Mastrangelo SVR, Dornte RW (1957) The system naphthalene–thianaphthene. Anal Chem 29:794–797

62. Kravchenko VM, Pastukhova IS (1958) The equilibrium of condensed phases in the naphthalene – thionaphtene system. Dokl Akad Nauk SSSR 119:285–287
63. Moerkens R, Bouwstra JA, Oonk HAJ (1983) The solid-liquid equilibrium in the system *p*-dichlorobenzene + *p*-bromochlorobenzene + *p*-dibromobenzene. Thermodynamic assessment of binary data and calculation of ternary equilibrium. Calphad 7:219–269
64. Oonk HAJ, Calvet MT, Cuevas-Diarte MA, Haget Y, van Miltenburg JC, Teunissen EH (1989) The system *p*-dibromobenzene + *p*-chloroiodobenzene + *p*-bromoiodobenzene–a methodological study on thermal analysis and thermodynamic phase-diagram analysis. Thermochim Acta 146:297–309
65. Stolk R, Rajabalee F, Jacobs MHG, Espeau P, Mondieig D, Oonk HAJ, Haget Y (1997) The RI-liquid equilibrium in the ternary system *n*-pentadecane + *n*-hexadecane + *n*-heptadecane. Calculation of liquidus surface and thermal windows comparison with experimental data. Calphad 21:401–410